Carbohydrate Polymers 99 (2014) 491–498

Contents lists available at ScienceDirect

Carbohydrate Polymers

journal homepage: www.elsevier.com/locate/carbpol

Extraction of agar from *Gelidium sesquipedale* (*Rodhopyta*) and surface characterization of agar based films

P. Guerrero, A. Etxabide, I. Leceta, M. Peñalba, K. de la Caba *

BIOMAT Research Group, University of the Basque Country (UPV/EHU), Polytechnic School, Donostia-San Sebastián, Spain

ARTICLE INFO

Article history:
Received 5 February 2013
Received in revised form 3 August 2013
Accepted 11 August 2013
Available online 27 August 2013

Keywords:
Gelidium
Agar
SPI
^{13}C NMR
XPS
FTIR
Thermo-moulding
Films

ABSTRACT

The chemical structure of the agar obtained from *Gelidium sesquipedale* (*Rhodophyta*) has been determined by ^{13}C nuclear magnetic resonance (^{13}C NMR) and Fourier transform infrared spectroscopy (FTIR). Agar (AG) films with different amounts of soy protein isolate (SPI) were prepared using a thermo-moulding method, and transparent and hydrophobic films were obtained and characterized. FTIR analysis provided a detailed description of the binding groups present in the films, such as carboxylic, hydroxyl and sulfonate groups, while the surface composition was examined using X-ray photoelectron spectroscopy (XPS). The changes observed by FTIR and XPS spectra suggested interactions between functional groups of agar and SPI. This is a novel approach to the characterization of agar-based films and provides knowledge about the compatibility of agar and soy protein for further investigation of the functional properties of biodegradable films based on these biopolymers.

1. Introduction

Interest in biodegradable polymers has increased recently in response to public concerns over the growing environmental problems caused by plastic waste after disposal and by depletion of non-renewable resources (Freile-Pelegrín et al., 2007). Therefore, biopolymers, natural polymers derived from renewable sources, such as polysaccharides, proteins, or lipids, are being used to produce biodegradable films (Fabra et al., 2009; Guerrero, Beatty, Kerry, & de la Caba, 2012; Leceta, Guerrero, Cabezudo, & de la Caba, 2013).

With regard to polysaccharides, the great variety of structures provides films with a wide range of properties. In this context, red marine seaweeds (*Rhodophyta*) are the source of some promising biopolymers since they contain considerable amount of the agar polysaccharide, which is a complex mixture of polysaccharides having the same backbone chain structure. In seaweeds, agar fulfils a function analogous to that of cellulose in terrestrial plants, although it differs because marine seaweeds require a more flexible structure to resist currents and waves motion (Rochas & Lahaye, 1989). Agar is a hydrophilic colloid consisting of polysaccharides that have the ability to form reversible gels simply by cooling a hot aqueous solution. It is composed of alternating 1,3-linked D-galactose and 1,4-linked 3,6 anhydro-L-galactose units. This disaccharide can be substituted by sulfate esters and methoxyl, and may also carry pyruvic acid residues (Duckworth & Yaphe, 1971). The type, amount, and location of these substitutes strongly affect the physical properties of the gel and therefore, its functionality (Freile-Pelegrín & Murano, 2005). Agar forms a slightly viscous solution after solubilization in hot water and then becomes a thermoreversible gel when the temperature is brought down. It could be an alternative source for biodegradable films since it shows high mechanical strength with moderate water resistance (Phan, Debeaufort, Voilley, & Luu, 2009; Wu, Geng, Chang, Yu, & Ma, 2009).

Soy protein is also a renewable polymer that can also be used in the manufacture of biodegradable films (Liu et al., 2010). Soy protein is the major coproduct of soy bean oil and it is readily available. Soy proteins are composed of a mixture of albumins and globulins, 90% of which are storage proteins with globular structure, consisting mainly in 7S and 11S globulins (Kinsella, 1979). The behaviour of proteins is determined by the amino acid composition, molecular size, and environment. Protein conformation also affects functionality; in globular proteins the more polar charged groups are oriented towards the surface. Moreover, non-covalent forces (hydrophobic interactions, hydrogen bonding, and electrostatic attractions) are involved in protein–protein and protein–solvent interactions, which influence the overall functional properties (Guerrero & de la Caba, 2010).

* Corresponding author. Tel.: +34 943017188.
E-mail address: koro.delacaba@ehu.es (K. de la Caba).

0144-8617/$ – see front matter © 2013 Elsevier Ltd. All rights reserved.
http://dx.doi.org/10.1016/j.carbpol.2013.08.049

Biodegradable films can be formed from a mixture of polysaccharides and proteins. The compatibility between the polysaccharide and the protein strongly affects the final properties of the film, thus the analysis of the functional groups present in both macromolecules provide a very helpful knowledge in order to understand the interaction between these two biopolymers. In this context, the agar extracted from *Gelidium sesquipedale* algae was characterized by ^{13}C NMR. There are several analytical procedures devoted to the characterization of agar, but ^{13}C NMR has been proved to be exceptionally fruitful and it is now the obligatory analysis for its characterization (Usov, 2011). The aim of this work was to prepare agar-based films with different soy protein contents and processed them by compression moulding. Functional groups of both biopolymers were identified by Fourier transform infrared (FTIR) spectroscopy and the surface composition of the agar-based films was investigated by X-ray photoelectron spectroscopy (XPS). There are many studies related to the elucidation of the chemical composition of biopolymers, but the study of surface composition by XPS is a novel approach in the field of biodegradable films. The objective of this preliminary work is focused on the interactions between agar and soy protein in order to optimize formulations and processing to prepare active packaging films. This first approach to the characterization of agar-based films could be greatly helpful not only for the identification of functional groups but also for the optimization of the composition to develop biodegradable films. The knowledge of the compatibility between biopolymers is necessary when a novel packaging film is designed. As far as we know, there are a vast number of research works about agar in the literature, but not about XPS characterization for agar-based films, thus the results showed in this work could help in making decisions when agar is used for the preparation of films. Although further investigation is necessary to optimize the film composition, the present work showed that agar-based films have a great potential as packaging films, which could contribute to the reduction of the use of raw materials from non-renewable sources, which is of great importance for industries, governments and consumers.

2. Materials and methods

2.1. Materials

The red algae *G. sesquipedale (Rodophyta)* used in his work, was collected on the northern coast of Spain (Hondarribia beach: 43°24′N, 01°47′W) in autumn (September). The samples were washed in fresh water to remove remaining sand and salt.

Soy protein isolate (SPI), PROFAM 974, with 90% minimum protein content on dry basis was obtained from ADM Protein Specialties Division, Netherlands. SPI has 5% moisture, 4% fat, and 5% ash and its isoelectric point is 4.6. The amino acid composition is given in a previous work (Guerrero, Stefani, Ruseckaite, & de la Caba, 2011). Glycerol, supplied by Panreac, was used as plasticizer.

2.2. Agar extraction

Agar extraction was carried out with distilled water. The dried sample (30 g) was immersed in boiling water (900 mL) for 4 h and the solution was separated from the residue by filtration on 50 μm blutex nylon. The solution was gelled at room temperature and then frozen at −25 °C. After that, the agar gel was freeze-dried to obtain the powder.

2.3. Preparation of films

Agar film forming solution was prepared by dissolving agar (5 g/150 mL) in distilled water (AG0SPI). Agar was replaced (25 and 50 wt%) by SPI to obtain agar–soy protein films (AG25SPI and AG50SPI, respectively). Glycerol was used as plasticizer (30% (w/w) of agar powder). Film forming solutions were prepared by mixing agar or agar–soy protein in distilled water, heating at 80 °C at 150 rpm on a magnetic stirrer for 30 min. After that, glycerol was added to the solutions, which were maintained at 80 °C for other 30 min under stirring at 150 rpm. The pH of solutions was appropriately adjusted to pH 10 with NaOH (0.1 M). Samples were freeze-dried using Alpha 1-4 LD freeze-dryer (Martin Chirst), and the powder was thermally compacted using a caver laboratory press (Atlas™). The powder was placed between two sheets of aluminium with a 100 mm diameter. These sheets were placed between the platens of the press, which had been previously heated to 150 °C. A pressure of 12 MPa was applied for 2 min and the platens were allowed to cool to room temperature before removing film samples. All films were conditioned in a controlled bio-chamber (ACS Sunrise 700 V) at 25 °C and 50% RH (relative humidity) for 48 h before testing.

2.4. Carbon 13 nuclear magnetic resonance (^{13}C NMR) spectroscopy

^{13}C NMR spectroscopy of agar was performed using 5% (w/v) of agar solution in D_2O and recorded at 90 °C on a Bruker Avance 500 MHz spectrometer, equipped with BBO z-gradient probe at base frequency of 125.75 MHz. The pulse sequence was submitted to a delay and acquisition time of 2 and 1.30 s. Data accumulations were performed at 14,000 scans.

2.5. Fourier transformed infrared (FTIR) spectroscopy

FTIR spectra of the films were carried out on a Nicolet Nexus FTIR spectrometer using ATR Golden Gate (Specac). A total of 32 scans were performed at 4 cm^{-1} resolution. Measurements were recorded between 4000 and 700 cm^{-1}.

2.6. Moisture content (MC)

Three specimens of each sample were weighed (m_w) and subsequently dried in an air-circulating oven at 105 °C for 24 h. After this time, samples were reweighed (m_0) to determine MC values. MC values were calculated as:

$$MC(\%) = \frac{m_w - m_0}{m_w} \times 100$$

2.7. X-ray photoelectron spectroscopy (XPS) analysis

XPS was performed in a SPECS spectrometer using a monochromatic radiation equipped with Al Kα (1486.6 eV). The binding energy was calibrated by Ag $3d_{5/2}$ peak at 368.28 eV. All spectra were recorded at 90° take-off angle. Survey spectra were recorded with 1.0 eV step and 40 eV analyser pass energy and the high resolution regions with 0.1 eV step and 20 eV pass energy. All core level spectra were referenced to the C 1s neutral carbon peak at 284.6 eV. Spectra were analysed using the CasaXPS 2.3.16 software, and peak areas were quantified with a Gaussian–Lorentzian fitting procedure.

2.8. Contact angle determination

A contact angle metre (model Oca20, dataphysics instruments) was used to perform contact angle measurements on the surface of films. A film sample (20 mm × 80 mm) was put on a movable sample stage and levelled horizontally; then, a drop of about 3 μL of distilled water was placed on the surface of the film using a microsyringe. The contact angle was measured in a conditioned room by

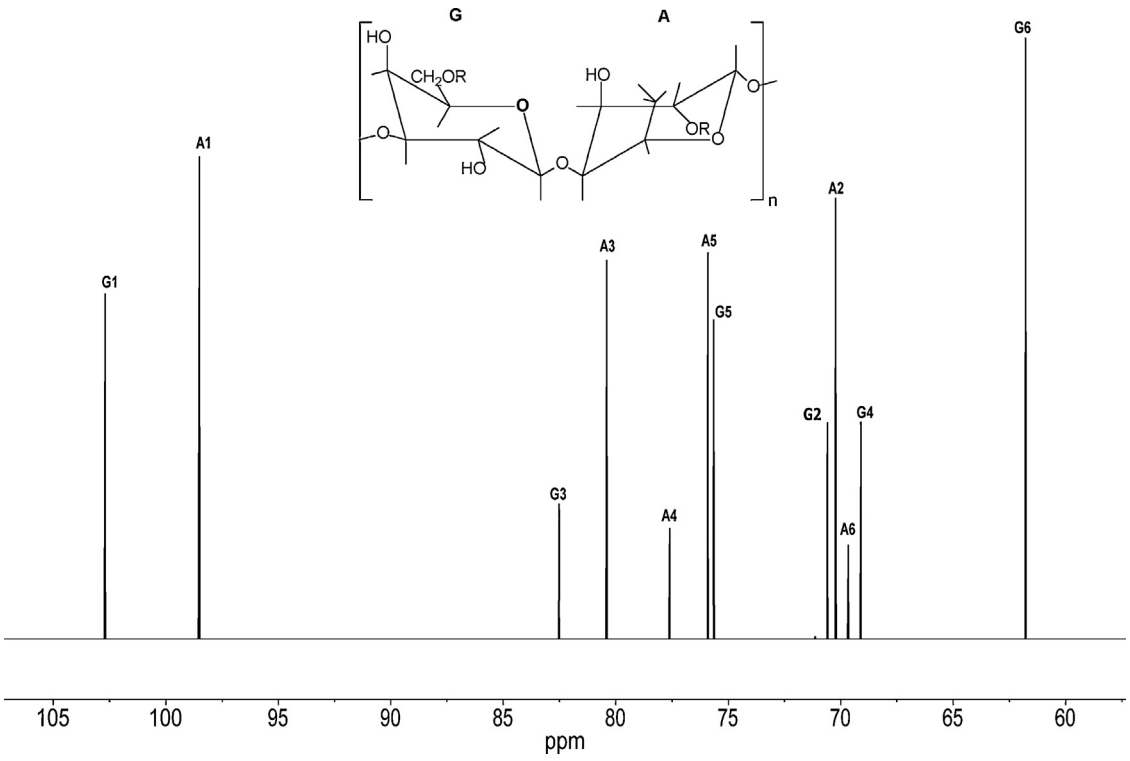

Fig. 1. ^{13}C NMR spectra of the agar extracted from *Gelidium sesquipedale*.

recording contact angle values. Image analyses were carried out using SCA20 software. Five replicates were made per formulation.

2.9. Gloss measurement

The gloss was measured at 60° incidence angles according to the ASTM D-523 (ASTM, 1999) using a flat surface gloss metre (Konika-Minolta Multi Gloss 268 plus). Measurements were taken in triplicate for each sample and three films of each formulation were considered. All the results were expressed as gloss units, relative to a highly polished surface of black glass standard with a value near to 100.

2.10. X-ray diffraction (XRD)

XRD studies were performed with a diffraction unit (PANalytical Xpert PRO) operating at 40 kV and 40 mA. The radiation was generated from a Cu-Kα ($\lambda = 1.5418$ Å) source. The diffraction data were collected from 2θ values from 2.5° to 50°, where θ is the angle of incidence of the X-ray beam on the sample.

2.11. Statistical analysis

Data were subjected to one-way analysis of variant (ANOVA) by means of a SPSS computer programme (SPSS Statistic 20.0). Post hoc multiple comparisons were determined by the Tukey's test with the level of significance set at $P < 0.05$.

3. Results and discussion

There are seasonal variations in thallus length, number of branches and fertile thalli in the *G. sesquipedale*, and the maximum percentage of fertile thalli was observed in September, but the agar composition was not affected by seasonal variations (Mouradi-Givernaud, Hassani, Givernaud, Lemione, & Benharbet, 1999). The main polysaccharide components of the red algae are sulfated galactans. It is now that sulfated galactans usually have a linear backbone built up of alternating 3-linked β-D-galactopyranose and 4-linked α-galactopyranose residues. In addition, 4-linked residues may be present as 3,6 anhydro-α-L-galactopyranose. Hence, there are different types of disaccharide repeating units in the molecules of galactans. Moreover, hydroxyl groups in these repeating units may be methylated, sulfated or substituted by single monosaccharide residues. There are several analytical procedures devoted to the characterization of sulfated galactans in such complex mixtures. ^{13}C NMR has been proved to be exceptionally fruitful and it is the obligatory analysis; furthermore, XRD can be used to confirm the structure of polysaccharides (Usov, 2011).

3.1. ^{13}C NMR and FTIR of the agar extracted from G. sesquipedale

The native agar obtained from *G. sesquipedale* had a golden colour. The ^{13}C NMR spectra of agar investigated are shown in 12 signals assigned to the carbon of agarobiose units as shown in Fig. 1. The spectra basic unit of agarose has the simple structure of a β-D-galactopyranose (G in Fig. 1) and 3,6 anhydro-α-L-galactopyranose (A in Fig. 1). Each residue contains six chemically different carbon atoms, which in the following will be named G1–G6 and A1–A6 for the galactopyranosyl and the anhydro galactopyranosyl, respectively.

^{13}C NMR spectra signals for each carbon atom in galactose are G1 at 102.7 ppm, G2 at 70.6 ppm, G3 at 82.5 ppm, G4 at 69.1 ppm, G5 at 75.6 ppm, and G6 at 61.8 ppm, whereas those for the carbon atoms in anhydro galactose are A1 at 98.5 ppm, A2 at 70.2 ppm, A3 at 80.4 ppm, A4 at 77.6 ppm, A5 at 75.9 ppm, and A6 at 69.7 ppm (Usov, Yarotsky, & Shashkov, 1980), similar to the ^{13}C NMR spectra of analogous polysaccharides (Flemming, Meyland, & Schaumburg, 1980; Usov, Ivaniva, & Shashkov, 1983). The absence of the peak at 59.1 ppm corresponding to O-methyl group indicates a lowly methylated agarose structure (Usov et al., 1983).

The FTIR spectrum for agar is shown in Fig. 2. The band at 3291 cm^{-1} is associated with OH groups, the absorbance

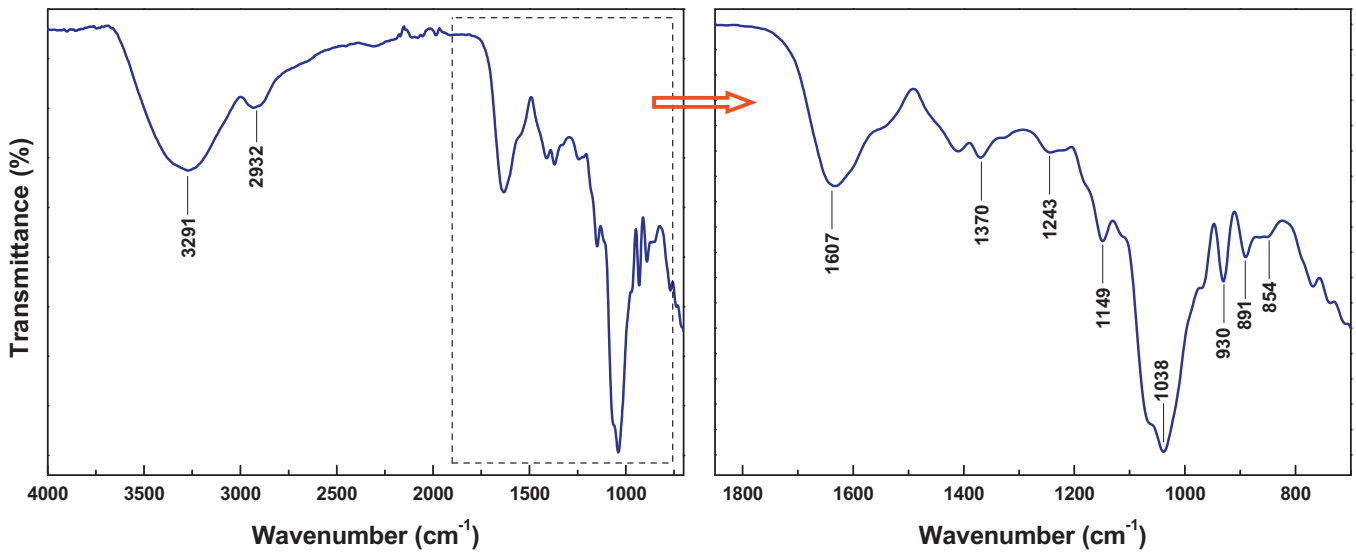

Fig. 2. FTIR spectra of the agar extracted from *Gelidium sesquipedale*.

at 2932 cm^{-1} with CH_2 groups, and the absence of significant absorbance at 2845 cm^{-1} indicates the very low methylation degree (O—CH_3) of the agar obtained, in agree with the ^{13}C NMR spectra. However, the band at 1607 cm^{-1}, assigned to amide I vibrations, indicates the presence of proteins.

The absorption bands at 1370 and 1243 cm^{-1} are due to the vibration mode of sulphate groups. These bands are related to the agar quality, because the presence of α-L-galactose 6-sulphate units decreases the gel strength of these polygalactans. The band at 1149 cm^{-1} is due to vibration mode of ester-sulphate link vibrations and the small signal at 854 cm^{-1} is assigned to the sulphate in C-4 from galactose (Gómez-Ordóñez & Rupérez, 2011; Melo, Feitosa, Freitas, & de Paula, 2002; Rochas, Lahaye, & Yaphe, 1986). Therefore, the FTIR spectrum indicates the presence of sulfation on C4 of β-D-galactopyranosyl.

The intense band observed at 1038 cm^{-1}, common to all polysaccharides, is mainly due to the coupling of the C—O or the C—C stretching modes with the C—O—H bending modes. The modes due to the C—O—C bridge of the 3,6 anhydro units, may also contribute at these frequencies, but the strong absorbance at 930 cm^{-1} is the one attributed to the vibration of the C—O—C bridge of 3,6-anhydrogalactose (Stancioff & Stanley, 1969). This band is the most representative of the agar family since the infrared spectra of the other polysaccharides contained in red algae, such as cellulose and xylans, do not exhibit absorptions at this wave numbers. This band has been correlated with the degree of sulphatation because the 1,4 linked residues may sometimes be substituted by sulphate groups on the C6 and replaced by the 3,6 anhydro α-L-galactose residue. Finally, the band at 891 cm^{-1} was attributed to skeletal mode due to β-D-galactose units in agar (Rajasulochana & Gunasekaran, 2009).

3.2. Characterization of agar-based films

Flexible agar and agar/SPI films were prepared by compression. All films were transparent and showed homogeneous structure. As shown in Table 1, moisture content increased ($P < 0.05$) with SPI content. In order to analyse the hydrophobic or hydrophilic character of the films, water contact angle values were determined. These values are higher when hydrophilicity is lower, thus the final state of the water drop on the film surface can be taken as an indication of surface wettability. Contact angle were determined for films with different content of SPI and the values are shown in Table 1. A contact angle of 81.5°, which is significantly high, was observed for agar films. The contact angle in AG0SPI and AG25SPI films remained constant and there was no significance difference ($P > 0.05$); however, contact angle values decreased ($P < 0.05$) to 40.1° for AG50SPI films. This behaviour indicates that AG–SPI interactions result in a high exposure of hydrophobic groups towards the surface in AG25SPI films, maintaining the hydrophobic character of AG0SPI films; however, higher contents of SPI substantially modify the surface of AG50SPI films.

Regarding surface properties, gloss describes the capacity of the surface to reflect direct light, and it is another parameter often used to evaluate the appearance of films surface. Table 1 presents the values of the films measured at 60°. In this case, the gloss of the films was dependent of SPI content and decreased ($P < 0.05$) with the addition of SPI, which was related to the surface morphology reached during the film formation. All the values were lower than 60°, considered as the standard of a glossy material (Atarés, De Jesús, Talens, & Chiralt, 2010), which means a very low gloss and a high surface roughness. This fact indicates that, at surface level, the addition of SPI in agar-based film promotes a rougher surface, thus decreasing the gloss.

3.3. Surface composition of the films

The surface analysis of agar films was performed using X-ray photoelectron spectroscopy (XPS). In Fig. 3, the survey scan of agar films is represented with the identification of the O 1s, N 1s, C 1s and Ca 2p peaks. The three predominant features were C 1s, O1s and N 1s, but very small peaks of Ca 2p and S 2p were also present in the survey spectra. Ca element was found around 1.5% and decreased below 1% when SPI content increased, and the content of S element was found below 1%. Consequently, the elements other than C, O, and N were neglected. Table 2 shows the peak area ratios observed for agar films surface. The ratio of the peak area of C 1s, O 1s, and

Table 1
Moisture content, contact angle and gloss values of AG0SPI, AG25SPI, and AG50SPI films.

Sample	MC (%)	Contac angle (°)	Gloss 60°
AG0SPI	15.64 ± 0.37[a]	81.51 ± 2.14[a]	14.81 ± 0.41[a]
AG25SPI	17.06 ± 0,17[b]	80.82 ± 2.82[a]	11.47 ± 1.42[b]
AG50SPI	16.39 ± 0.32[b]	40.13 ± 1.88[b]	9.88 ± 1.85[c]

[a–c]Two means followed by the same letter in the same column are not significantly ($P > 0.05$) different through the Tukey's multiple range test.

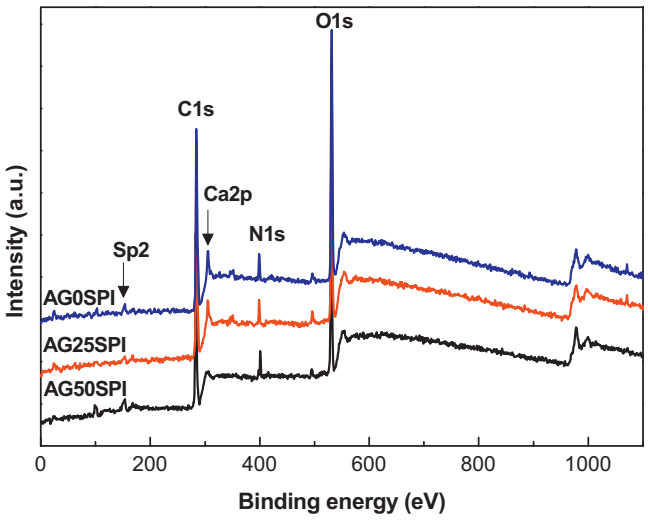

Fig. 3. XPS survey spectra of AG0SPI, AG25SPI, and AG50SPI films.

N 1s, O/C and N/C, roughly reflects the ratio of the concentration of these atoms in the agar films surface. By comparing C, O, and N percentages in the surface of films, it can be said that the C percentage increased, while the O percentage decreased when SPI content increased, indicating that the specific surface area of the films was different. Different factors contributed to the different distribution of C, O, and N in the surface of films. The water localized could bring about strong interactions with the charged groups on surface. These interactions might increase the effect of hydrogen-bonding, which caused the change of the band frequency of C and O atoms on the surface of samples (Zhao et al., 2011). The interactions of agar and SPI could change not only the surface structure of the films, but also the band frequency in XPS spectra. The O/C atom ratio changed from 0.59 to 0.45 for AG0SPI to AG50SPI films, indicating that the addition of SPI decreased the oxidation. No significant difference was found in the N/C ratios of the films, indicating that the amino groups exposed do not change.

The functional groups present on the surface were identified by the C, N, and O peaks (Gaiani et al., 2006). The binding energies and areas of these functional groups were accomplished by performing XPS. C 1s, N 1s, and O 1s spectra for the films surface are presented in Figs. 4–6.

3.3.1. Carbon speciation by XPS

The spectrum curve of C element for each individual samples is further deconvoluted to illustrate the C status in the sample. The C 1s peak was decomposed in three peaks (Fig. 4) corresponding to the C1 (C—C/C—H), C2 (C—O/C—N), and C3 (O—C=O) functions (Azioune et al., 2005). The major component C1 appeared at 284.4–284.7 eV due to the hydrocarbons and C—C bonding present in the protein. C2 band represented the bonds in 285.9–286.4 eV binding energy range, in agreement with literature (Gaiani et al., 2006). The carboxyl group, C3, was found at 288.7–288.1 eV, similar to the literature values (Rubio et al., 2002). The variation in absorption peaks reflects the change in the content of C element among samples. The binding area of C1 and C2 in AG0SPI films was lower than in AG25SPI and AG50SPI films, which is in agreement with the contact angle values shown in Table 1. C1 indicates the hydrophobic character of the surface, and C2 and C3 reveal the content of active functional groups in agar films, which benefits the wettability of bonding surfaces. The variation of the C3 peak shows that amination may occur between polysaccharides and proteins during the film forming. The similarity of C 1s peaks shape in Fig. 4a–c indicates the similar distribution of the oxygen present on the surface of the films. It is also worth to note that the form and position of the line in the spectra did not change. The results indicated that the addition of SPI could result in the lost of oxygenated organic species; this was consistent with the decrease of the O/C ratio from 0.59 to 0.45 shown in Table 2.

Table 2
Compositional information obtained using X-ray photoelectron spectroscopy.

Sample	C (at.%)	O (at.%)	N (at.%)	Ca (at.%)	S (at.%)	O/C	N/C
AG0SPI	60.8	35.7	2.1	1.4	0.1	0.59	0.03
AG25SPI	63.5	32.9	2.6	0.7	0.2	0.52	0.04
AG50SPI	66.2	29.9	3.3	0.2	0.2	0.45	0.05

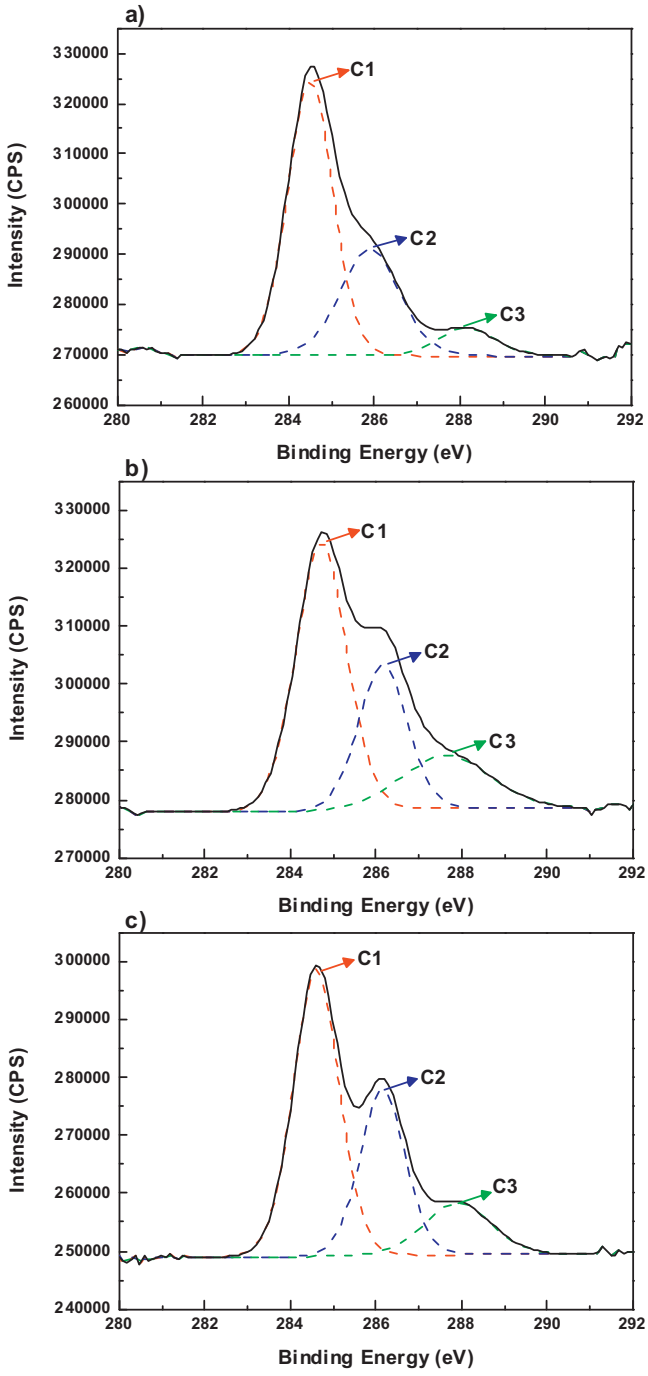

Fig. 4. XPS of C 1s features of (a) AG0SPI, (b) AG25SPI, and (c) AG50SPI films.

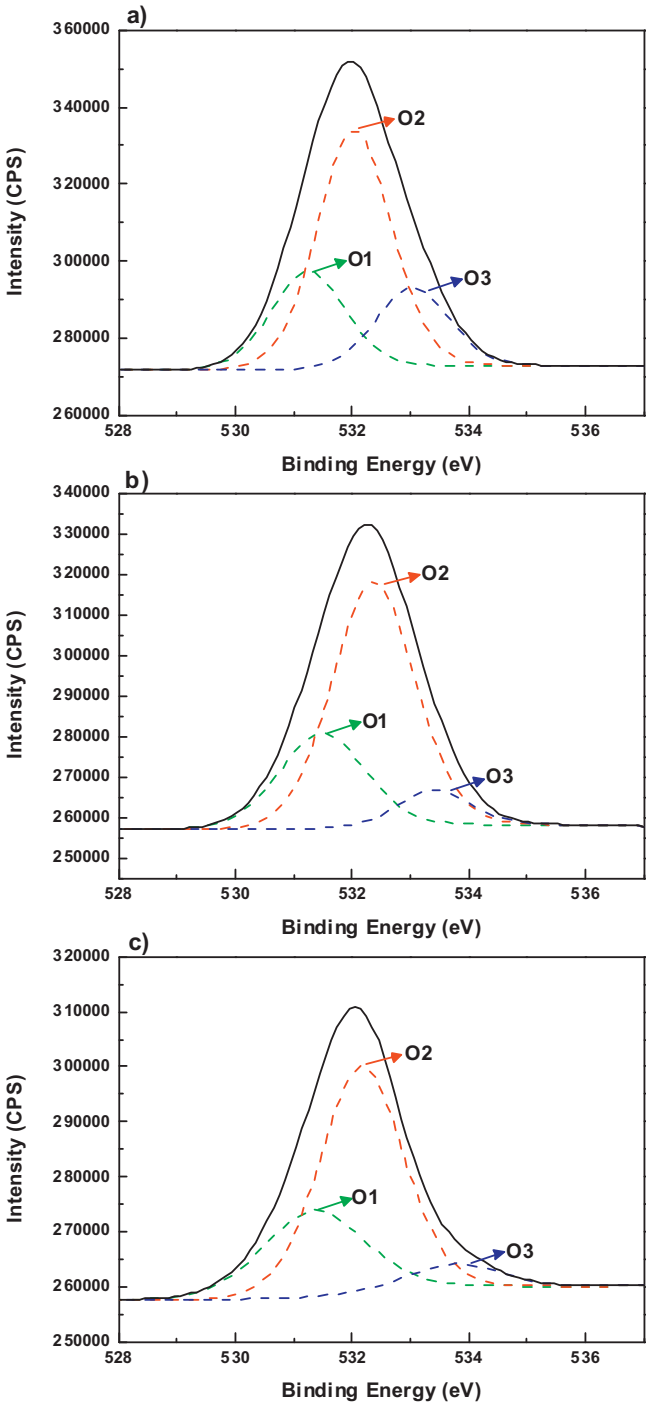

Fig. 5. XPS of O 1s features of (a) AG0SPI, (b) AG25SPI, and (c) AG50SPI films.

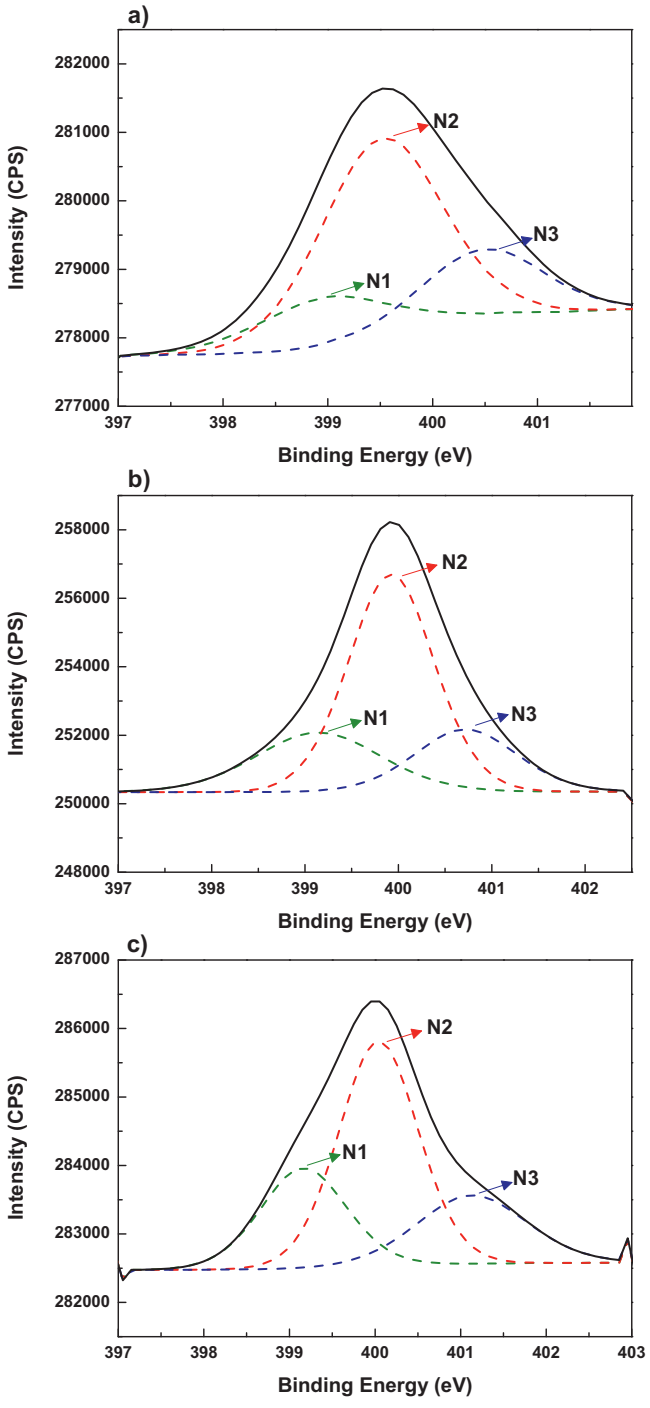

Fig. 6. XPS of N 1s features of (a) AG0SPI, (b) AG25SPI, and (c) AG50SPI films.

3.3.2. *Oxygen speciation by XPS*

The O 1s features in Fig. 5 have similar shape and binding energy, indicating that the oxygen containing species on all the samples were similar. Generally, the O 1s spectra do not provide much information about chemical state because many O containing species are present (Zhao et al., 2011), but in order to obtain useful information, the O 1s peak was decomposed (Fig. 5a–c). There are three peaks, corresponding to the O1 (O—C=O/O=C—N), O2 (C—O—C/C—OH) and O3 (H_2O) functions. The major component, O2, appeared at 532.0–532.5 eV, O1 was identified in 531.1–531.6 eV binding energy range, and O3 was found at 533.0–533.8 eV. As can be seen in Table 2, the content of O element decreased significantly and that of N element increased slightly, indicating that O element micromolecules may have been produced in SPI films under a high temperature process. The results suggested that C—O—C and C—OH bonds were dominant.

3.3.3. *Nitrogen speciation by XPS*

The N 1s peak was decomposed in three peaks (Fig. 6a–c) corresponding to the N1 (N—H/N—C), N2 (C=N/N—C), and N3 (H—N—C(O)O/N—C=C) functions. The major component N2 was at 399.5–400.1 eV, N1 was identified in the 398.7–399.3 eV binding energy range, and N3 was found at 400.5–4001.1 eV. The shape of all N 1s peaks was similar. The comparison of the N 1s binding area

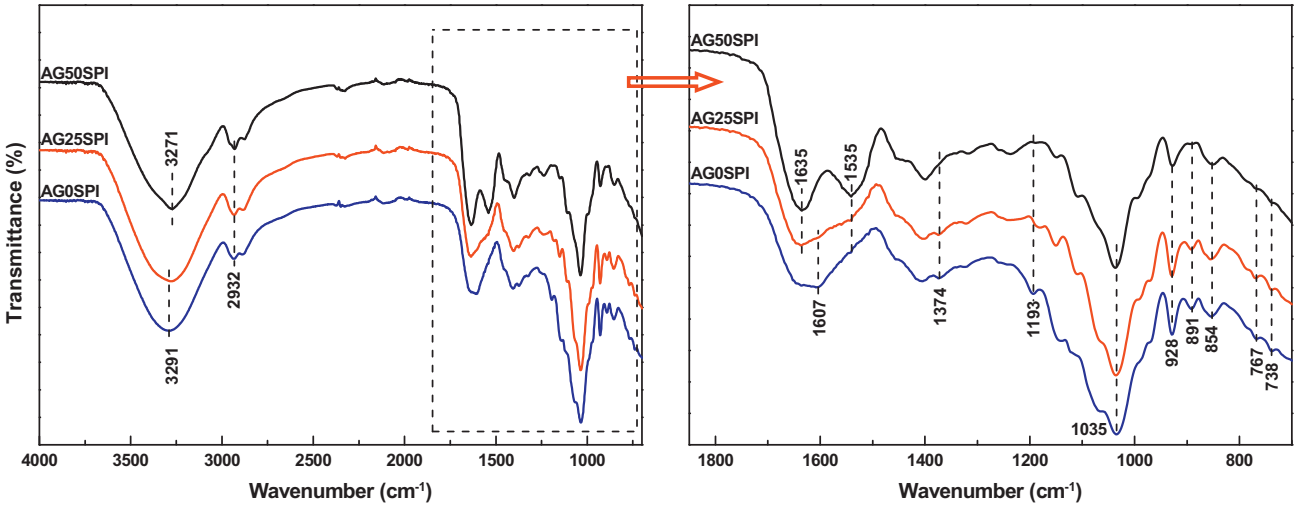

Fig. 7. FTIR spectra of AG0SPI, AG25SPI, and AG50SPI films.

of AG0SPI, AG25SPI, and AG50SPI films showed that the binding area of N 1s increased with SPI, indicating the exposure of amino groups towards surface. The reason may be due to the fact that the interaction between the protein and the polysaccharide decreased with a high content of protein.

3.4. FTIR spectra of the films

To better understand the results related to surface composition, the films were analysed by FTIR. Fig. 7 shows the FTIR spectra of AG0SPI, AG25SPI, and AG50SPI. The agar spectrum illustrated the stretching vibration of O—H and N—H functional groups, indicating that there is a great potential for intermolecular hydrogen bonds among hydroxyl groups, among amino groups, and between hydroxyl and amino groups. The large absorption band at 3291 cm^{-1} represents the O—H stretching and deformation band. The peak observed at 2932 cm^{-1} refers to the C—H stretching band. The weak peak at 2888 cm^{-1} is associated with methoxyl groups. The spectrum also shows a peak at 1607 cm^{-1}, corresponding to the C=O of the carboxylic group present in agaropectine. When SPI is incorporated, the main absorption bands of peptide linkage are related to C=O stretching at 1635 cm^{-1} (amide I), N—H bending at 1535 cm^{-1} (amide II) and C—H deformation at 1400 cm^{-1} appears (Guerrero et al., 2011). The absorption bands at 1374 and 854 cm^{-1} are due to vibration mode of sulphate groups. The intense band observed at 1035 cm^{-1} is mainly due to the coupling of the C—O or C—C stretching modes with the C—O—H bending modes. The absorption bands at 891 and 928 cm^{-1} are attributed to galactose units in agar. Finally, the contribution of glycerol appears in the bands at 853, 929, and 1035 cm^{-1}.

After the addition of SPI, the functional groups of AG0SPI films exhibited changes in the FTIR spectra. The absorption band at 1607 cm^{-1}, corresponding to carboxylic group in agar, moved to 1635 cm^{-1} and its intensity increased, and the band at 1541 cm^{-1} (amide II) only appeared in AG50SPI film, indicating the high content of SPI. The bands at 1374, 1193, and 891 cm^{-1}, attributed to vibration mode of sulphate groups, disappeared with the addition of SPI. The band at 1035 cm^{-1} decreased notably with the incorporation of SPI. Therefore, the characteristic agar bands showed changes in intensity with the incorporation of SPI. These results suggested that the hydrogen bonding interactions existed between agar and soy protein. The interactions became stronger from AG0SPI to AG25SPI films because SPI may act as a reinforcing agent, forming a compact and homogeneous three dimensional network gel prior to setting of the film. However, AG50SPI films probably decreased intermolecular interactions among agar molecules, causing aggregations.

3.5. X-ray diffraction (XRD)

In order to analyse the change in the structure of agar-based films and to determine the degree of crystallinity, X-ray diffraction patterns of the films with different soy protein contents were studied and are shown in Fig. 8. All diffractograms show a broad diffuse band centred at about $2\theta = 20^{\circ}$ and two peak with small intensity at $2\theta = 14.5^{\circ}$ and 32.4°. When soy protein content was high, it can be observed that the intensity of the broad band decreased, which means that the degree of structural order also decreased. However, AG0SPI and AG25SPI samples showed similar structure because the small peaks at $2\theta = 14.5^{\circ}$ and 32.4° and the broad peak at $2\theta = 20^{\circ}$ were maintained, while in AG50SPI film, the small peaks disappeared and the main broad peak at $2\theta = 20^{\circ}$ decreased in intensity and increased in wideness, which would be indicative of AG–SPI interactions, as it was shown by FTIR analysis.

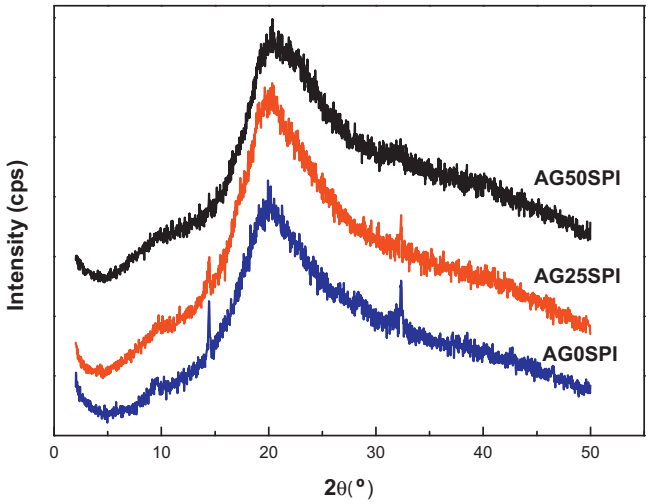

Fig. 8. X-ray diffraction spectra of AG0SPI, AG25SPI, and AG50SPI films.

4. Conclusions

The results of this study confirmed the potential of the agar obtained from *G. sesquipedale* to prepare biodegradable films with good functional properties for packaging applications since the films are homogeneous, transparent, and flexible. Moreover, the characterization of agar-based films carried out by XPS and FTIR spectroscopy provides essential and complementary information to allow a better understanding of the films. It has been seen that the incorporation of SPI produces changes on the surface of agar-based films, such as the orientation of the hydrophobic groups and hydrogen bonding interactions between agar and SPI, which influence functional properties. The results obtained in this work suggest that SPI contents lower than 25% could be adequate to prepare films with good functional properties due to the interactions between polysaccharides and proteins that could promote the formation of a compact and reinforced three dimensional network.

Acknowledgements

The authors thank the University of the Basque Country UPV/EHU (research group GIU12/06 and project PES11/35) as well as the Basque Government (SAIOTEK programme 2012–2013) for their financial support. Itsaso Leceta thanks the Basque Government (fellowship BFI-2010-82). Thanks also Advanced Research Facilities (SGIker) from the UPV/EHU.

References

ASTM D523-99 (1999). Standard test method for specular gloss. In *Annual book of ASTM standards*. Philadelphia, PA: American Society for Testing and Materials.

Atarés, L., De Jesús, C., Talens, P., & Chiralt, A. (2010). Characterization of SPI based edible films incorporated with cinnamon or ginger essential oils. *Journal of Food Engineering*, *99*, 384–391.

Azioune, A., Siroti, F., Tanguy, J., Jouini, M., Chehimia, M. M., Miksa, B., et al. (2005). Interactions and conformational changes of human serum albumin at the surface of electrochemically synthesized thin polypyrrole films. *Electrochimica Acta*, *50*, 1661–1667.

Duckworth, M., & Yaphe, W. (1971). The structure of agar. Part I. Fractionation of a complex mixture of polysaccharides. *Carbohydrate Research*, *16*, 189–197.

Fabra, M. J., Hambleton, A., Talens, P., Debeaufort, F., Chiralt, A., & Voilley, A. (2009). Influence of interactions on water and aroma permeabilities of i-carrageenan-oleic acid-beeswax films used for flavor encapsulation. *Carbohydrate Polymers*, *76*, 325–332.

Flemming, M., Meyland, I., & Schaumburg, K. (1980). ^{13}C NMR spectra at 67.9 MHz of aqueous solutions of agarose and partly 6-O-methylated agarose at 95 °C. *Acta Chemica Scandinavica, B*, *34*, 103–107.

Freile-Pelegrín, Y., Madera-Santana, T., Robledo, D., Veleva, L., Quintana, P., & Azamar, J. A. (2007). Degradation of agar films in humid tropical climate: Thermal, mechanical, morphological and structural changes. *Polymer Degradation and Stability*, *92*, 244–252.

Freile-Pelegrín, Y., & Murano, E. (2005). Agars from three species of *Gracilaria* (*Rhodaphyta*) from Yucatan peninsula. *Bioresource Technology*, *96*, 295–302.

Gaiani, C., Ehrhardt, J. J., Scher, J., Hardy, J., Desobry, S., & Banon, S. (2006). Surface composition of dairy powders observed by X-ray photoelectron spectroscopy and effects on their rehydration properties. *Colloids Surfaces B: Biointerfaces*, *49*, 71–78.

Gómez-Ordóñez, E., & Rupérez, P. (2011). FTIR-ATR spectroscopy as a tool for polysaccharide identification in edible brown and red seaweeds. *Food Hydrocolloids*, *25*, 1514–1520.

Guerrero, P., Beatty, E., Kerry, J. P., & de la Caba, K. (2012). Extrusion of soy protein with gelatin and sugars at low moisture content. *Journal of Food Engineering*, *110*, 53–59.

Guerrero, P., & de la Caba, K. (2010). Thermal and mechanical properties of soy protein films processed at different pH by compression. *Journal of Food Engineering*, *100*, 261–269.

Guerrero, P., Stefani, P. M., Ruseckaite, R. A., & de la Caba, K. (2011). Functional properties of films based on soy protein isolate and gelatin processed by compression. *Journal of Food Engineering*, *105*, 65–72.

Kinsella, J. E. (1979). Functional properties of soy proteins. *Journal of the American Oil Chemists' Society*, *56*, 242–258.

Leceta, I., Guerrero, P., Cabezudo, S., & de la Caba, K. (2013). Environmental assessment of chitosan-based films. *Journal of Cleaner Production*, *41*, 312–318.

Liu, D., Chen, H., Chang, P. R., Wu, Q., Li, K. N., & Guan, L. (2010). Biomimetic soy protein nanocomposites with calcium carbonate crystalline arrays for use as wood adhesive. *Bioresource Technology*, *101*, 6235–6241.

Melo, M. R. S., Feitosa, J. P. A., Freitas, A. L. P., & de Paula, R. C. M. (2002). Isolation and characterization of soluble sulfated polysaccharide from the red seaweed *Gracilaria cornea*. *Carbohydrate Polymers*, *49*, 491–498.

Mouradi-Givernaud, A., Hassani, L. A., Givernaud, T., Lemione, Y., & Benharbet, O. (1999). Biology and agar composition of *Gelidium sesquipedale* harvested along the Atlantic coast of Maroco. *Hydrobiologia*, *399*, 391–395.

Phan, T. D., Debeaufort, F., Voilley, A., & Luu, D. (2009). Biopolymer interactions affect the functional properties of edible films based on agar, cassava and arabinoxylan blends. *Journal of Food Engineering*, *90*, 548–558.

Rajasulochana, N., & Gunasekaran, S. (2009). Fourier transform infrared spectral analysis of agars of *Gelidium micropterum* and *Gracilaria fergusonii*. *Asian Journal of Chemistry*, *21*, 4543–4546.

Rochas, C., & Lahaye, M. (1989). Average molecular weight and molecular weight distribution of agarose and agarose-type polysaccharides. *Carbohydrate Polymers*, *10*, 289–298.

Rochas, C., Lahaye, M., & Yaphe, W. (1986). Sulfate content of corrageenan and agar determined by infrared spectroscopy. *Botanica Marina*, *29*, 335–340.

Rubio, C., Costa, D., Bellon-Fontaine, M. N., Relkin, P., Pradier, C. M., & Marcus, P. (2002). Characterization of bovine serum albumin adsorption on chromium and AISI 304 stainless steel, consequences for the *Pseudomonas fragi* K1 adhesion. *Colloids and Surfaces B: Biointerfaces*, *24*, 193–205.

Stancioff, D. J., & Stanley, N. F. (1969). Infrared and chemical studies of algal polysaccharides. *Proceedings of the International Seaweed Symposium*, *6*, 595–609.

Usov, A. I. (2011). Polysaccharides of the red algae. *Advances in Carbohydrate Chemistry and Biochemistry*, *65*, 115–217.

Usov, A. I., Ivaniva, E. G., & Shashkov, A. S. (1983). Polysaccharides of algae XXXIII: Isolation and ^{13}C NMR spectral study of some new gel forming polysaccharides from Japan sea red seaweeds. *Botanica Marina*, *XXVI*, 285–294.

Usov, A. I., Yarotsky, S. V., & Shashkov, A. S. (1980). ^{13}C NMR spectroscopy of red algal galactans. *Biopolymers*, *19*, 977–990.

Wu, Y., Geng, F., Chang, P. R., Yu, J., & Ma, X. (2009). Effect of agar on microstructure and performance of potato starch film. *Carbohydrate Polymers*, *76*, 299–304.

Zhao, X. Y., Chen, J., Zhu, Q. J., Du, F., Ao, Q., & Liu, J. (2011). Surface characterization of 7S and 11S globulin powders from soy protein examined by X-ray photoelectron spectroscopy and scanning electron. *Colloids and Surfaces B: Biointerfaces*, *86*, 260–266.